



New infrared spectroscopy instrument for reliable low humidity water vapour isotopic composition measurements

Mathieu Casado¹, Amaelle Landais¹, Tim Stoltmann², Justin Chaillot¹, Mathieu Daëron¹, Frédéric Prié¹, Baptiste Bordet², Samir Kassi²

- 5 ¹ Laboratoire des Sciences du Climat et de l'Environnement, CEA–CNRS–UVSQ–Paris-Saclay–IPSL, Gif-sur-Yvette, France
² LiPHY, Laboratoire Interdisciplinaire de Physique, Université Grenoble Alpes / CNRS, Grenoble, France

Correspondence to: Mathieu Casado (mathieu.casado@gmail.com)

10 **Abstract.** In situ measurements of water vapour isotopic composition in Polar Regions has provided needed constrains of post-deposition processes involved in the archiving of the climatic signal in ice core records. During polar winter, the temperatures are so low that current commercial techniques are not able to measure the vapour isotopic composition with enough precision. Here, we make use of new developments in infrared spectroscopy and combine an optical feedback frequency stabilised laser source (OFFS technique) using a V-shaped optical cavity (VCOF) and a high-finesse cavity ring down cavity (CRDS) which
15 yield sufficient precision to measure isotopic composition at water mixing ratios down to 1 ppmv. Indeed, thanks to the stabilisation of the laser by the VCOF, the instrument suffers extremely low drift and very high signal to noise ratio. Using new constrains on the fitting technique, the instrument is additionally not hindered by a large isotope-humidity response which at low humidity can create extensive biases on commercial instruments.

1 Introduction

20 Water isotopic composition is commonly used as an atmospheric tracer (Galewsky et al., 2016) or in paleoclimate studies (Casado, 2018; Jouzel and Masson-Delmotte, 2010). Indeed, water stable isotopes concentrations are modified throughout the hydrological cycle (Dansgaard, 1964), in particular at each phase transitions (Craig and Gordon, 1965; Majoube, 1971; Merlivat and Nief, 1967), heavier isotopes are preferentially found in the condensed phase rather than the vapour (Jouzel, 2010). This property is paramount to the isotopic paleothermometer (Dansgaard, 1964; Lorius et al., 1969) which links the
25 variations of isotopic composition in an ice core record to past temperatures (EPICA, 2004; North Greenland Ice Core Project members, 2004). While the isotopic paleothermometer is generally admitted to be a reliable paleoclimate proxy (Jouzel and Masson-Delmotte, 2010), in low accumulation regions, complex post-deposition processes (Casado et al., 2018; Ekaykin et al., 2002) can modify the recorded signal (Casado et al., 2021; Steen-Larsen et al., 2014) and limit the interpretation as a past temperature record (Casado et al., 2020; Laepple et al., 2018).

30



Studying water vapour isotopic composition in polar regions (Casado et al., 2016; Steen-Larsen et al., 2013) is key to a comprehensive understanding of the processes affecting water isotopes in cold, dry environment, usually characterised by low accumulation (Berkelhammer et al., 2016; Bonne et al., 2019; Bréant et al., 2019; Casado et al., 2018; Ritter et al., 2016). However, in the low accumulation regions of the poles, vapour monitoring of isotopic composition is sparse (Wei et al., 2019) and for the coldest sites limited to summer. Indeed, these measurements are mostly based on commercial instruments (Steig et al., 2014) for which the precision drops dramatically for humidity levels below 100 ppmv (Leroy-Dos Santos et al., 2021). In general, the amount of sublimation and condensation is poorly known during the winter months (Genthon et al., 2016), and there is no instrument able to monitor the atmospheric vapour isotopic composition due to the extremely low humidities (below 100 ppmv) (Casado et al., 2016; Ritter et al., 2016), despite attempts for new generation of infrared spectrometers which were able in laboratory environments to reach humidity as low as 20 ppmv (Landsberg et al., 2014). At the site of Dome C, where the longest ice core has been drilled, humidity levels below 100 ppmv are found 79% of the year, and below 20ppm, 56% of the year (Genthon et al., 2022), yielding an urgent need for vapour isotopic composition monitoring able to measure in conditions as dry as 1ppm.

Applications of infrared spectroscopy techniques to trace detection and isotopic monitoring is dominated by two techniques: Optical-Feedback Cavity Enhanced Absorption Spectroscopy (OF-CEAS) (Landsberg, 2014) and Cavity Ring Down Spectroscopy (CRDS) (Romanini et al., 1997; Steig et al., 2014). The interest of the former is to use optical feedback (Laurent et al., 1989) to stabilise and refine the laser source and measure the absorption features associated to molecular transitions in a high finesse resonating cavity (Morville et al., 2005). The latter on the other hand takes advantage of the extreme sensitivity of the CRDS technique (Čermák et al., 2018) to generate very precise absorption spectroscopy.

Here, building up on recent efforts to combine the advantages of both techniques (Burkart and Kassi, 2015; Chaillot et al., 2023; Stoltmann et al., 2017), we present a new generation of infrared spectrometers able to measure water isotopic composition at extremely low humidities (less than 1ppmv, or equivalent to a water pressure of 0.06Pa). These conditions are indeed commonly found in central Antarctica during the long polar winters where temperature can reach -90°C , but are also potentially found in the stratosphere or in other planets. This new generation of instrument, called VCOF-CRDS, is able to reach precision of 0.01‰ for monitoring vapour $\delta^{18}\text{O}$ in Central Antarctic conditions, as well as to maintain satisfactory performances at humidity around 1 ppmv. Overall, the new instrument achieves a precision roughly 20 times better than available commercial instruments, as well as a stability 20 times longer. An ingenious auto-referencing of the instruments also limits the impact of long term drift of the laser and reduce the need for drift correction through regular calibration.

2. Methods and instrumental setup

2.1. Description of the instrument

The new instrument is based on Optical Feedback Frequency Stabilisation (OFFS) Cavity Ring Down Spectroscopy (CRDS), a technique developed for CO₂ isotope monitoring (Burkart et al., 2014; Stoltmann et al., 2017) and transferred here to water isotopic composition measurement. It includes three modules: a laser source, a frequency scanner, and a gas analyser (see Figure 1).

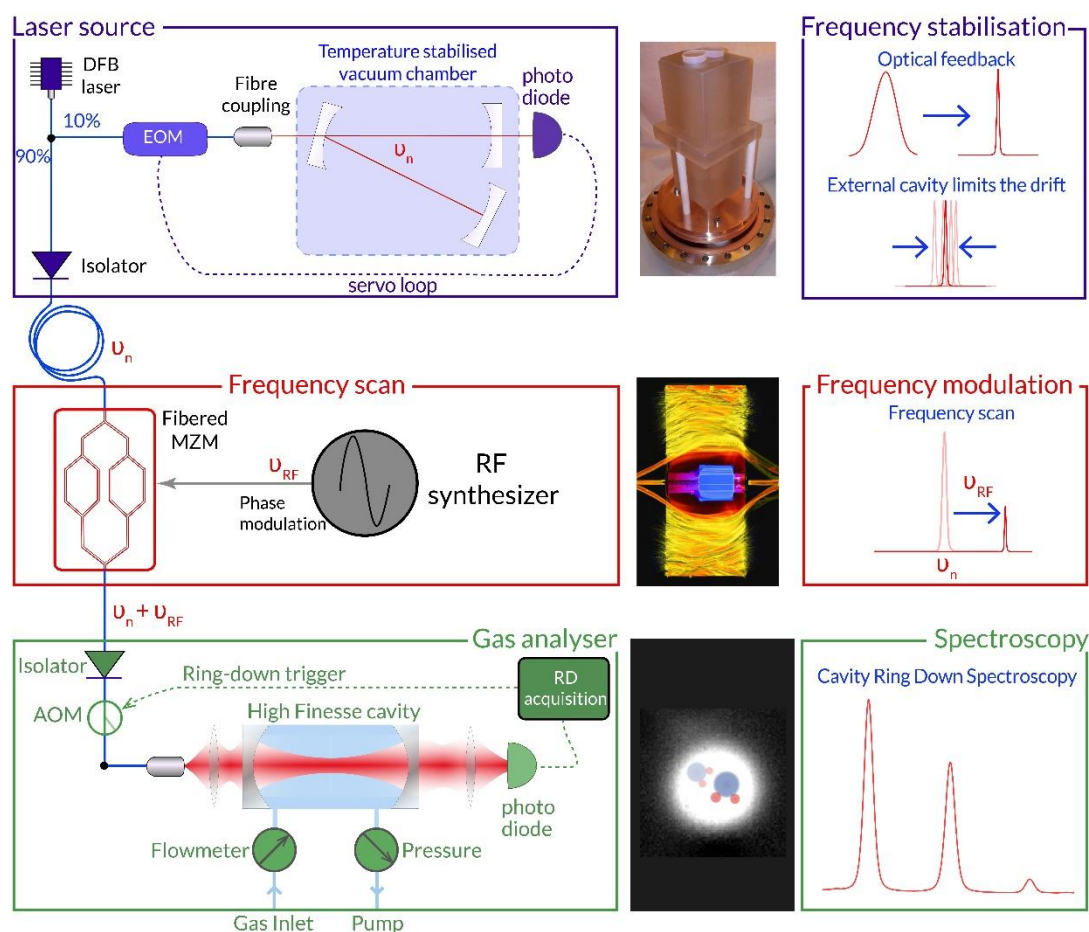


Figure 1: Experimental setup schematics: upper panel, the laser source, a picture of the monobloc zerodur V-shape stabilisation cavity, and the impact of the optical cavity on the linewidth and the drift of the laser source; middle panel, frequency scanner through a MZM, AI-generated representation of a MZM; bottom panel, the CRDS cavity used to analyse the gas, silhouette of two water molecules drawn on top of an IR picture of the mode of the cavity, and a schematic spectrum for the considered transition line (see Fig. 2).



75 The light source is primarily composed of a fibered Distributed FeedBack diode (DFB) stabilised by optical feedback in a monoblock Zerodur V-shaped cavity with a finesse of 131000. The frequency stabilisation leads to the narrowing of the linewidth of the crude DFB diode from a few MHz to less than 70 Hz, with a drift below 2 Hz s^{-1} (Casado et al., 2022). The long term drift in particular drops below 1 Hz s^{-1} , and is dominated by the aging of the zerodur glass (Jobert et al., 2022) providing from a spectroscopy point of view long term stability of the instrument, and thus, reducing the need for calibration
80 to compensate the drift.

The frequency scanner relies on a fibered Mach-Zehnder Modulator (MZM) (Izutsu et al., 1981) which enables to tune the frequency of the light source while preserving its spectral purity (Burkart et al., 2013). We apply an electrical radio-frequency signal to shift the sidebands generated by the MZM, and set up the polarisation so only a single sideband is preserved while
85 the other and the carrier are destroyed by negative interferences. The remaining power is around 0.9mW, and we use a fibered optical amplifier to increase the power to 11mW.

The light is then injected into a second cavity which is used for monitoring the isotopic composition of the water vapour based on Cavity Ring Down Spectroscopy (CRDS). The CRDS cavity consist of a 48 cm long copper cylinder, with a diameter of 7
90 cm in which a hole of 0.8 cm has been drilled over the full length. The reflectivity of the mirrors is 0.99995, leading to a finesse of 300 000. The length of the CRDS cavity can be ever so slightly adjusted by a piezo ceramic actuator which moves one of the mirror. This is used to adjust the length of the CRDS cavity, and thus its resonance frequency, to match the frequency of the light injected. The gas is injected in the cavity using Bronkhorst pressure and flow controllers. The cavity is maintained at a pressure of 35 mbar ($\pm 0.01\text{mbar}$), and the flow at 25 sccm to limit turbulences within the air flow.

95 **2.2. Spectroscopic analysis**

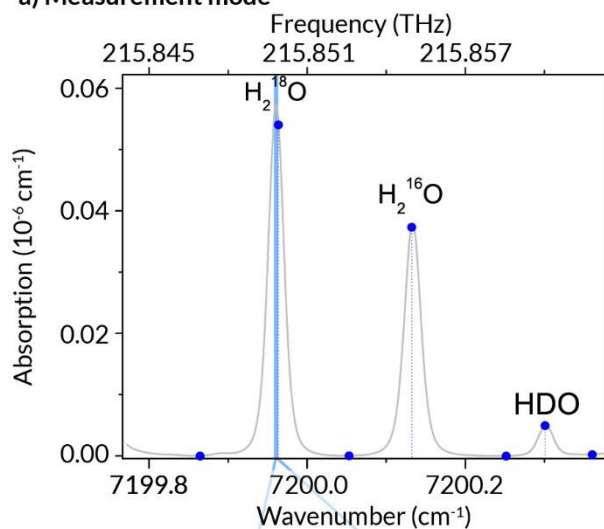
The instrument is set so the laser source produces a very stable light at exactly 7199.7 cm^{-1} , the frequency of which is then shifted using solely the MZM. The instrument can then be used in two ways: slow full spectrum mode and high pace measurement mode.

100 At high spectral resolution, the instrument can be used to realise spectroscopy studies (Kassi et al., 2018), with performances of 10^{-12} cm^{-1} . Here, we use the instrument instead as a tool to monitor water vapour isotopic, in which case the pace of the measurement is key in order to avoid the gas concentration changing during the course of a spectrum. Instead of realising spectra including a large number of datapoint, in this case, we opt out for a large number of spectra with few datapoints at the most relevant frequencies to characterise the absorption lines. This is done by “jumping” of exactly one FSR of the CRDS
105 cavity using the MZM. With this approach, the spectral resolution is of only multiple of the FSR (around 297 MHz), but relocking is instantaneous. The interest of this technique compared to higher resolution scans, which are slower but also potentially more precise, is to prevent the gas composition to change during the duration of a scan. Fast variations of humidity

level during a scan creates large uncertainty in the fitting procedure which lead to additional noise which are not averaged out due to their auto-correlated features. The high pace scans are associated with noise with little auto-correlation which can be averaged out rapidly.

110

a) Measurement mode



b) Frequency referencing

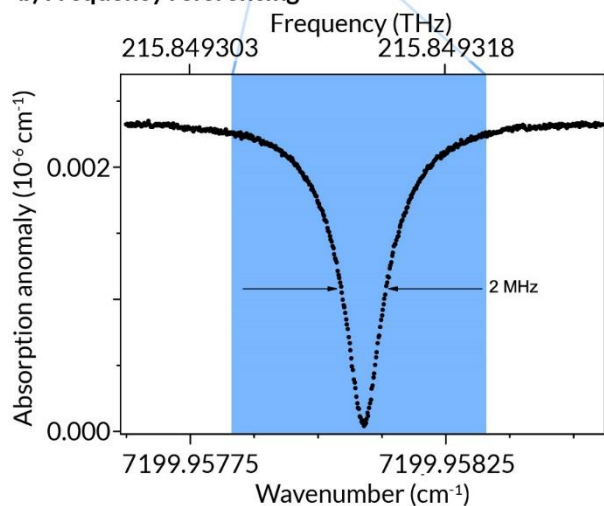


Figure 2: Absorption spectra realised by the new instrument: a) in measurement mode: high resolution for reference spectra (grey points), parking method for measurement high pace measurements (blue points) and illustration of the area scanned for frequency referencing (blue shaded area); b) in frequency referencing mode: feature of a Lamb dip saturated absorption pattern used to evaluate the drift of the instrument when deployed in the field where comb assisted spectroscopy is not possible.

115

In the high pace measurement mode, the spectra are composed of 7 datapoints (one at the top of each transition, and four for the baseline, Fig. 2a) and are realised in 0.7 s. The absorption profile is fitted using a speed-dependent Nelkin-Ghatak profile



(SDNGP) (Long et al., 2011), similarly to the approach used to measure CO₂ isotopic composition (Stoltmann et al., 2017).
120 The typical standard deviation of the fit residuals is around $2 \times 10^{-12} \text{ cm}^{-1}$, leading to a signal to noise ratio of the order of
10 000.

2.3. Frequency referencing

Even though the drift of the laser source is extremely limited (below 2 Hz s^{-1}), at the scale of several hours, this can lead to
significant deviations of the frequency, which lead to drift of the measured isotopic composition. This issue is general for
125 infrared spectrometers and is usually tackled by *a posteriori* drift correction of the isotopic composition itself (Leroy-Dos
Santos et al., 2021). Traditionally, the frequency of the VCOF has been locked on an optical frequency comb locked itself on
the GPS signal (Gotti et al., 2018). Here, we propose instead to measure a Lamb dip saturated absorption feature to counteract
the drift of the laser source. Indeed, at low pressure, the number of molecules can be so low that a *dip* feature appears at the
centre of saturated absorption transitions (Fig. 2b) (Burkart et al., 2015; Kassi et al., 2018). These features are characterised
130 with very small linewidth (below 20 kHz if the pressure is low enough), and their frequency being a physical constant, can be
used as a frequency reference.

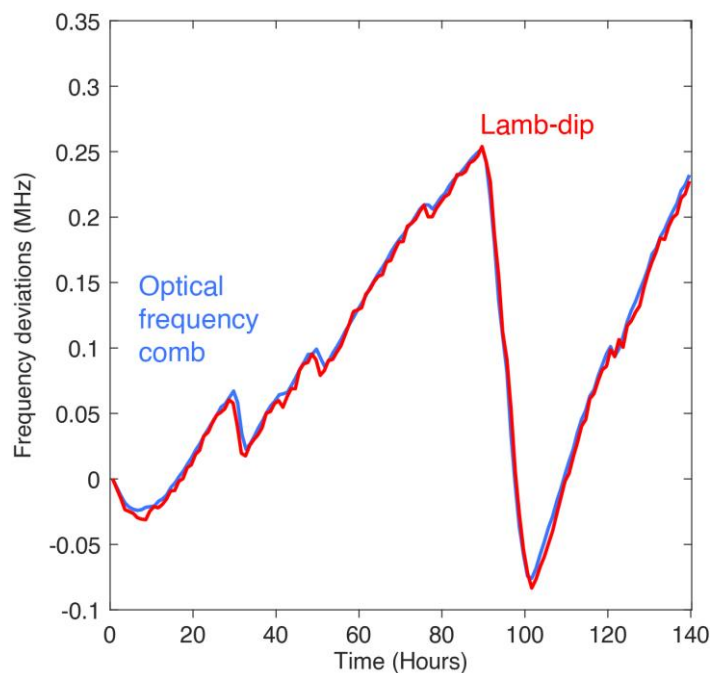


Figure 3: Frequency deviation of the laser source as measured from the beatnote of the laser with an optical frequency comb
135 (blue, (Burkart et al., 2014)) compared to measurement from the centre of a lamb-dip saturated absorption feature (red, (Kassi
et al., 2018))



Here, we make use of this property to evaluate the frequency drift of the laser source by scanning every hour the Lamb dip feature associated with the H_2^{18}O transition at 7199.96cm^{-1} . To do so, we decrease the pressure inside the cavity down to 0.1 mBar, let the cavity stabilise to this new experimental conditions for 2 minutes, and measure Lamb dip feature at extremely high resolution for 7 minutes. This method provides with frequency measurements of the Lamb dip feature centre with a precision of 2.5 kHz in a single scan (Kassi et al., 2018). The frequency deviation measured from the Lamb dip method reproduces exactly the ones estimated from the measurement of a beatnote with an optical frequency comb locked on a GPS (Burkart et al., 2014) (Fig. 3), with a correlation between the two times series of $r^2 = 0.995$ ($p < 0.05$). We used this measurement of the deviation of the frequency of the laser source as a self-referencing method which can be applied every hour to ensure that the deviation of the laser source frequency remains smaller than 10 kHz.

3. Results

We separate the performances of the instrument with first, the precision and the drift of the instrument in the long term, from the accuracy of the instrument of humidity to isotope relationship, and finally highlight the results of the frequency auto-referencing on the performances of the instrument.

3.1. Precision and drift

The new instrument precision has been evaluated by measuring water standards at various humidity levels generated by the calibration device described in (Leroy-Dos Santos et al., 2021). To evaluate the performances of the new technique directly, and not be impacted by the potential drift of the laser source, we used an optical frequency comb referenced to a GPS system to actively correct the frequency drift of the laser source. The impact of drift and mitigation by the frequency auto-referencing scheme are detailed in section 3.3. We generated repeated injections of the same water samples at the same conditions to generate water as stable as possible that is measured by the new instrument continuously. Typically, at 400 ppmv, this resulted in successive water level stable levels lasting up to 10 hours, followed by a drop of the humidity to refill the syringe (Fig. A1). The instrument then needs up to 1 hour to generate stable water again. This leads to time series of stable vapour content that can last several days but include gaps. We modified the traditional calculation of Allan variance to take gaps into account to calculate the precision as well as the drift of the instrument in a range of humidity from 20 to 1500 ppmv.

To evaluate both the short and long term stability of the signal, we monitored a constant humidity level of 400 ppmv for 7 days (Fig. 4a)). At the resolution of the instrument (3 Hz), the precision is roughly 0.2‰ in $\delta^{18}\text{O}$ at a humidity of 400 ppmv, and below 0.1‰ at 1 Hz. In these conditions, a Picarro L2130i in HDO mode only reaches precision of 2‰ at 1 Hz (Casado et al., 2016). The Allan standard deviation follows a normal law (characterised by a $1/\sqrt{N}$ decrease) until approximately 150 seconds when a limit value of roughly 0.01‰ in $\delta^{18}\text{O}$ variations is reached. The precision remains at this lowest value for duration longer than 2 days. Similarly, for d-excess, the instantaneous precision at 400 ppmv is roughly 2‰, and drops to 0.1‰ after



170 order isotopic compositions (Annex B) lead to an Allan standard deviation of d-excess characterised with excess noise compared to both the Allan standard deviations of $\delta^{18}\text{O}$ and δD (Figure B1). The fundamental flicker noise limit (flat Allan deviation for time larger than 2 minutes) could either be linked with the instable gas generation (variable humidity and pressure) or with the measurement technique itself. At low humidity (25 ppmv), more correlated noise appears, with a decrease of the Allan standard deviation not following the $1/\sqrt{N}$ law. After 1 minute, a precision of 0.2 ‰ in $\delta^{18}\text{O}$ is reached and maintained
175 for scales longer than 1 day (we chose not to interpret the drop after 6 hours below 0.1‰, as it is only visible in the last two points of the Allan standard deviation). Similarly, the instantaneous precision (1 second) of the instrument in d-excess at low humidity is very large (around 10‰) and slow drops to 2‰ around 1 minute.

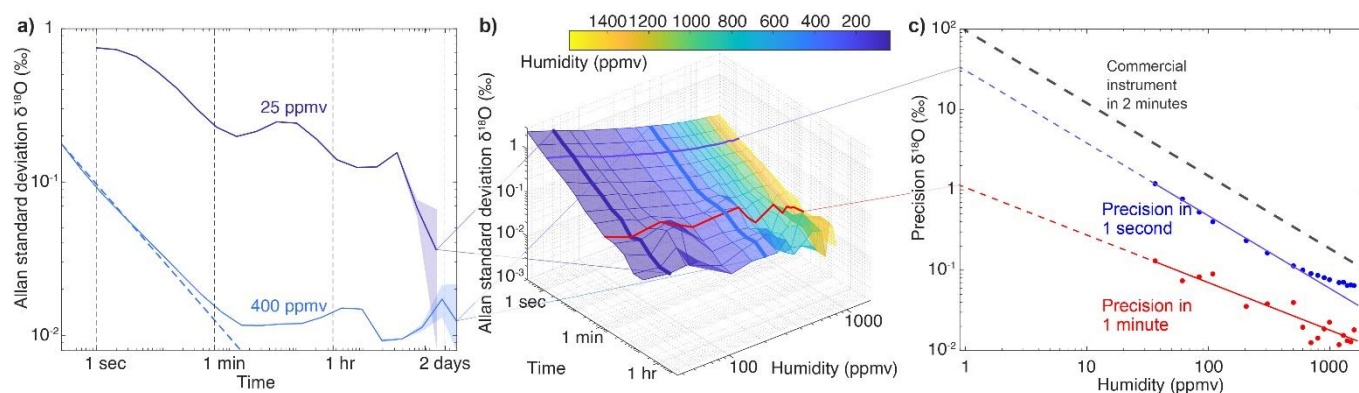
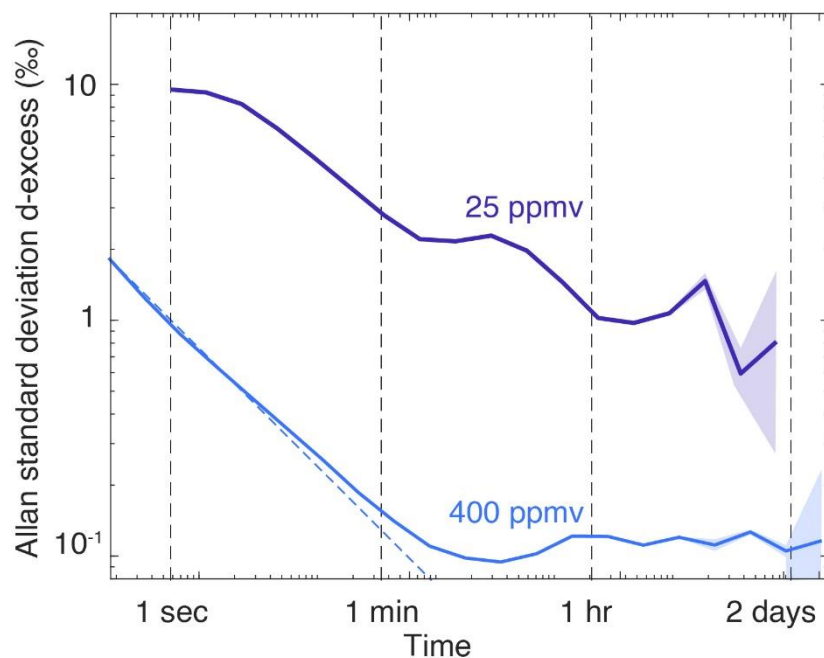


Figure 4: Allan standard deviation plots of the $\delta^{18}\text{O}$ measurements of the new instruments stabilised with an optical frequency comb: a) long-term Allan standard deviation plots realised at humidity levels of 25 and 400 ppmv with stable measurements of 7 days, b) 3D plot of the Allan standard deviation for different time scales and humidity levels, and c) evaluation of the precision of the instrument across humidity levels (dots) for measurements average over 1 second (blue), 1 minute (red), as well as fit with a power law (solid line) and extrapolation from the fit at lower humidities that could not be reached with the calibration device (Leroy-Dos Santos et al., 2021), compared to typical commercial instrument behaviour (dashed grey line, linear approximation of the performances of a Picarro L2140i extracted from Fig. 3 of (Leroy-Dos Santos et al., 2021) and of a Picarro L2130i from (Casado et al., 2016)).

The change of precision scales with humidity as shown in Figure 4c, and so at 1 Hz, the precision of the instrument at 30 ppmv is roughly 2‰ in $\delta^{18}\text{O}$ (roughly 10 times larger since the humidity is approximately ten times smaller), dropping down to 0.1‰ after 800 seconds, and at 800ppmv around 0.1‰ at 1 Hz and dropping to 0.005‰ after 800 seconds. While we were no able to generate stable moisture flux at 1 ppmv using the humidity generated described in (Leroy-Dos Santos et al., 2021), we extrapolated the precision expected after 1 minute at humidity lower than 25 ppmv by fitting the data with a power law and find a precision of 1‰ at roughly 1 ppmv.



195 **Figure 5:** Same as Figure 4a) for the d-excess: long-term Allan standard deviation plots realised at humidity levels of 25 and 400 ppmv with stable measurements of 7 days.

3.2. Accuracy of the instrument

Infrared spectrometers tend to be biased and require calibration for the dependency of their measurements with respect to change of humidity and isotopic composition itself. In this section, we illustrate the behaviour of the new infrared spectrometer
200 for varying humidity levels. We show a nearly flat humidity response till humidities around 200ppmv (Figure 6).

Infrared spectrometers usually have an isotopic response of the measurements to change of humidity levels that needs to be corrected with an appropriate instrument (Leroy-Dos Santos et al., 2021; Weng et al., 2020). Weng et al, (2020) suggested that the humidity response of the measurement of the isotopic composition, in particular the fact that this response is different for
205 different isotopic composition, is linked with spectroscopic effects in Picarro instruments (Grey lines in Fig. 6), rather than background humidity or memory effects, at least at the first order. Here, we show that the improved frequency stabilisation and the new fit parameters provide a much flatter isotope-humidity response, for both $\delta^{18}\text{O}$ and d-excess. The amplitude of the isotopic-humidity calibration changes is indeed one of the largest limitations to interpret vapour isotopic composition at low humidity conditions, as detailed by (Casado et al., 2016; Leroy - Dos Santos et al., 2020). In particular, in Antarctica where
210 humidity falls below 500ppmv frequently, the correction applied to $\delta^{18}\text{O}$ and d-excess (at 100ppmv, up to 15 and 100‰, respectively) can be one order of magnitude larger than the signal (diurnal cycle around 5 and 10‰, respectively at Dome C



(Casado et al., 2016)). Here, the amplitude of the correction remains below 1 and 10%, respectively, for humidities larger than 100ppmv.

215

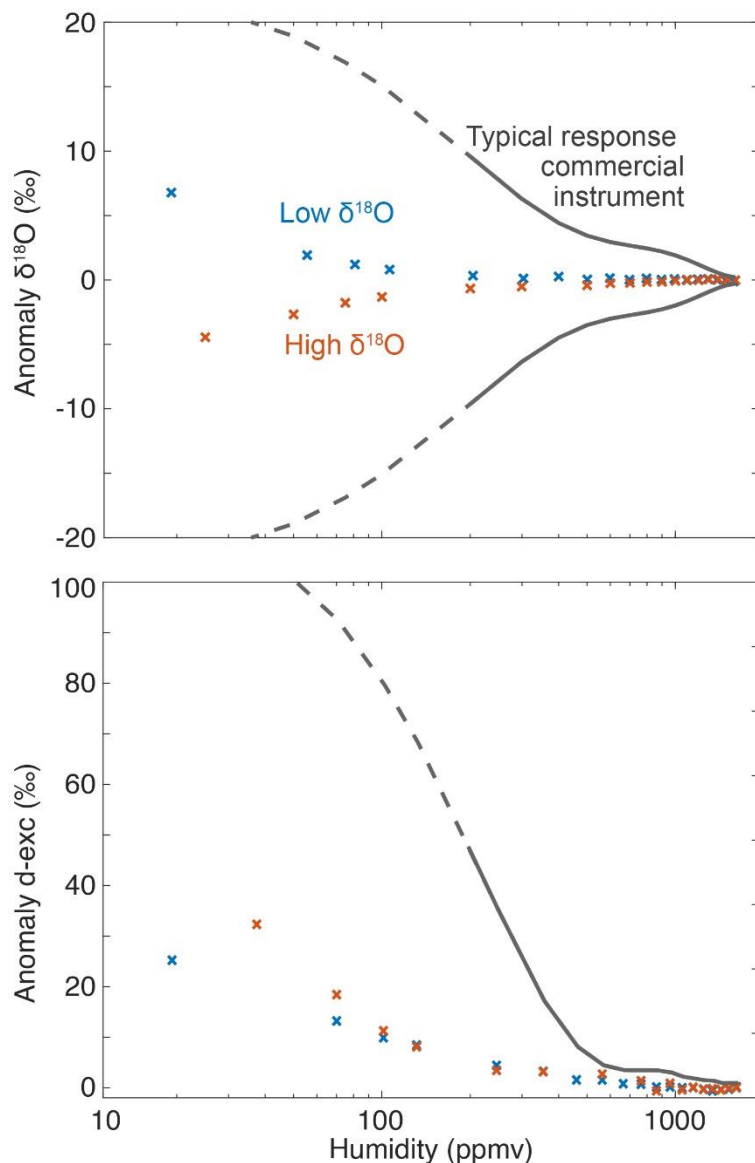


Figure 6: Isotope-humidity dependence for several isotopic compositions: evaluation of the anomalous measurement of a) $\delta^{18}\text{O}$ and b) d-excess for local tap distilled tap water (high $\delta^{18}\text{O}$, approximately of -7.5‰, orange) and depleted Antarctic water (low $\delta^{18}\text{O}$, approximately of -50.6‰, blue) compared to typical response from a commercial instrument at low humidity



220 (grey lines, extracted from the equations 4 and 5 in (Leroy-Dos Santos et al., 2021), based on a Picarro L2140i, full line:
humidity range where the regression was made from the observations, dashed line, extrapolation).

3.3. Frequency auto-referencing

225 The main source of uncertainty for the measurement comes from the drift of the laser source. Indeed, since the frequency scan
is only used to reach successive resonance mode of the CRDS cavity, the spectra produced in high pace measurement mode
are not necessarily exactly aligned with the absorption lines. For the current cavity, with a FSR of 297 MHz, it was not possible
to have datapoints exactly on top of all three scanned transitions, and in particular, the spectral point for the H₂¹⁸O transition
is relatively far from the transition centre (Fig. 7d).

230 We evaluated the impact of frequency drift on the measurement uncertainty by artificially adding frequency detuning during
the frequency scanning system measuring the same gas in stable conditions. The added detuning of the frequency ranged from
-100 to +100 MHz with a 50MHz resolution, as well as every 1MHz between -10 and +10MHz (Fig. 7a, c and e). For the HDO
transition where the measurement point was the closest to the transition centre, we observe no impact of the frequency detuning.
For the humidity measurement, a small impact is observed (around 0.1ppmv MHz⁻¹) linked to the small distance of the
235 spectroscopic measurement to the centre of the absorption feature. The main impact for our current setup is on δ¹⁸O for which
a sensitivity to drift of roughly 1.4‰ MHz⁻¹ is observed. Considering the current performances of the laser source (1.7 Hz s⁻¹,
(Casado et al., 2022)), this leads to a drift of the δ¹⁸O of roughly 0.008‰ per hour, or up to 0.2‰ per day. This is much larger
than the performances obtained in Figure 4a) at time scales longer than one hour which suggests that at long time scales, this
would be the dominating source of uncertainty.

240

In order to maintain the performances around 0.01‰ for δ¹⁸O for averages longer than two minutes, we need to include
frequency referencing every hour. We implemented the frequency auto-referencing mode described in Section 2.3. and
measured every hour Lamb dip features. The frequency drift of the laser source measured by this technique was then
compensated directly in the frequency modulation by the MZM. Note that no extrapolation of future drift is implemented, so
245 the frequency added on the frequency modulation is a step which is updated every hour when a new Lamb dip is measured.

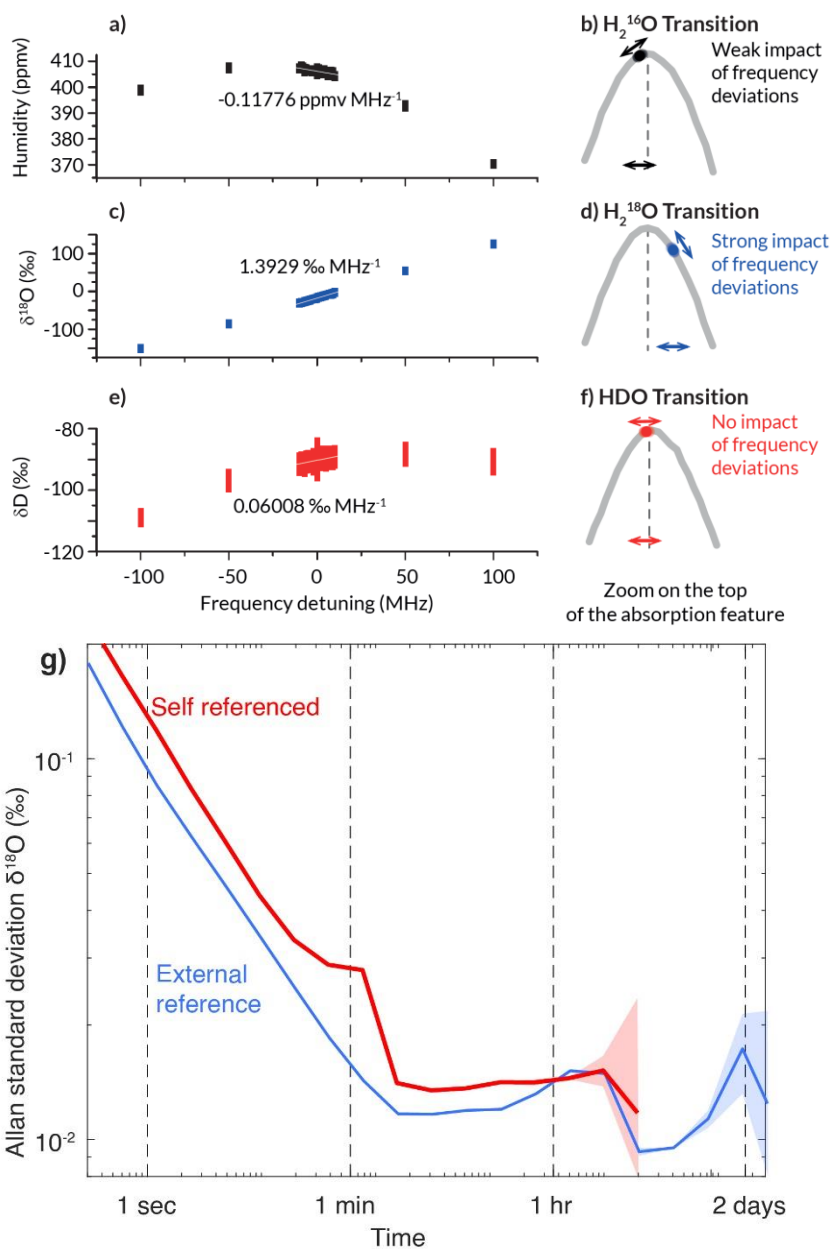


Figure 7: Evaluation of the impact of the frequency drift of the laser source on the measurements of isotopic composition: impact of the frequency detuning on the measured a) humidity, c) $\delta^{18}\text{O}$, and e) d-excess with illustration of the position of spectroscopic measurement point compared to their respective transition centre b), d), and f); Allan standard deviation of $\delta^{18}\text{O}$ for the instrument being self-referenced (red) and with an external frequency reference (blue) at 400ppmv.

250



We compare the Allan standard deviation of measurement of a constant sample made with this self-referenced mode of the instrument with the Allan standard deviation with the external frequency reference (Fig. 7g). For time scales shorter than one hour, an excess noise is added to the data, probably due to the step approach to correct the drift. An extrapolation from a given number of the previous Lamb dip measurement could potentially on average fix part of this excess noise, but with the risk of over-correction when the environmental conditions shift. Since despite this excess noise, a satisfactory precision can be reached after 5 minutes, this has not been implemented. For time scales longer than one hour, the performances of the instrument with the self-referencing are matching exactly the ones with external frequency referencing. The measurement of δD is not affected as the measurement point is perfectly centred on the transition.

Changing the length of the CRDS cavity to 23 cm would enable to mitigate a large part of the drift impact on $\delta^{18}O$ by aligning the measurement points with the centre of all three absorption features. This solution will be favoured for instrument deployed to the field, and would limit the need to implement frequency auto-referencing to every 6 hours.

4. Discussions

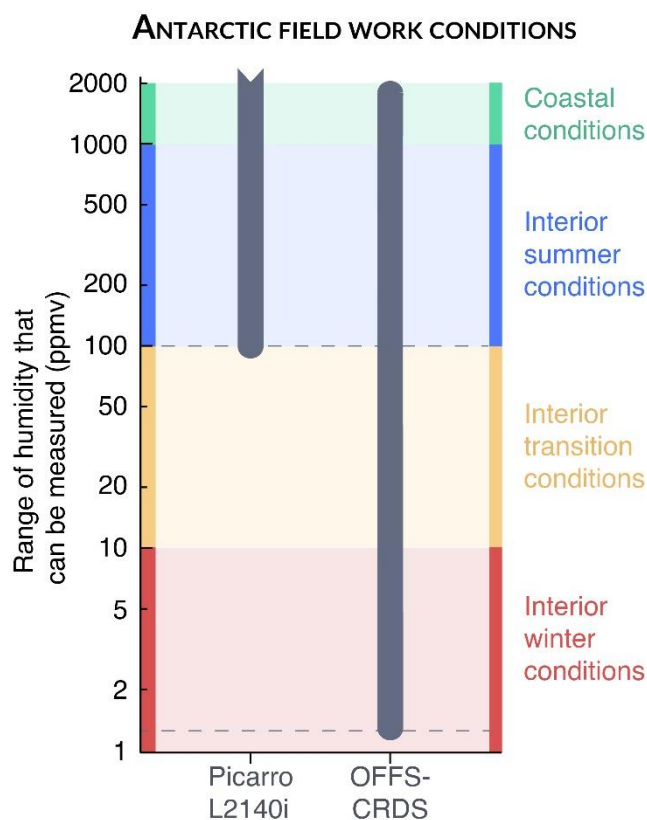
Major limitations arising from the capacity of infrared spectrometers to measure the isotopic composition at low humidities include water vapour monitoring in very cold field conditions, as well as evaluation of the fractionation coefficients of heavy isotopes with respect to light isotopes.

Current commercial instruments are limited to measure isotopic composition at humidity levels above 100 ppmv (Casado et al., 2016; Leroy-Dos Santos et al., 2021; Ritter et al., 2016). In general, this limits the application of the instruments to locations where the temperature is above $-40^{\circ}C$, and successful deployments has been reported in a large number of Arctic field campaigns (Akers et al., 2020; Bonne et al., 2014; Leroy - Dos Santos et al., 2020; Steen-Larsen et al., 2013), on vessels in Polar regions (Kurita et al., 2015; Thurnherr et al., 2020), and even in coastal areas in Antarctica (Bagheri Dastgerdi et al., 2021; Bréant et al., 2019). Inland Antarctica, some campaign provided with vapour isotopic composition monitoring but were limited to the warmest summer conditions (Casado et al., 2016; Ritter et al., 2016).

Developing infrared spectrometers able to yield satisfactory precision at low humidities has been attempted in the past, making use of high sensitivity of OFCEAS techniques (Landsberg et al., 2014) but deployment to Antarctica field station was never successful due to the strong impact of slow drifting fringes which induced significant drift after a couple of hours (Casado, 2016; Landsberg, 2014). The new instrument presented here and based on OFFS-CRDS show potential to measure at humidity levels 100 times lower (Figure 8). It should be able to measure 95% of the time at the deep interior station Concordia (located at Dome C) where winter temperatures are usually around $-80^{\circ}C$ (Genthon et al., 2021). Combining the stability of the frequency stabilised laser source (OFFS and Lamb dip frequency referencing) and the high precision and stability of CRDS



technique, the new instrument can circumvent all the hurdles that limit the monitoring of water vapour isotopic composition monitoring in the coldest conditions, such as found in Antarctica in winter.



290 **Figure 8:** Range of humidities at which the new instrument can measure isotopic composition with a precision better than 1‰.

The current instrument cannot be deployed to the field due to its size and weight (1 m³, 230kg), the fragility of the VCOF source (the glass cavity is suspended by fragile ceramic rods, vacuum must be maintained), and the bulkiness and the frailty of the control electronics (instruments must be extremely isolated for static shocks due to the lack of electric ground with the thick ice layer). The performances of the instrument in the field should be roughly the same, provided that the temperature stabilisation of the instrument is as good as in the AC rooms of the lab. Indeed, the proof of concept for the frequency auto-referencing shows that the instrument will not suffer drift associated with change of the laser source wavelength.

300 The determination of physical parameters associated with the different heavy isotopes is also limited with instrumental capabilities. Indeed, currently, several studies attempted to measure the fractionation associated with gaseous solid phase transitions and ended with contradictory results at temperature below -30°C (Ellehoj et al., 2013; Lamb et al., 2017; Majoube,



1971). Better determinations of these fractionation coefficients are key for isotope enabled climate models (Risi et al., 2008; Werner et al., 2011) which use these parametrisation throughout the water cycle, with temperature often much lower than -
305 30°C, especially in high altitude cloud microphysics processes.

4. Conclusion

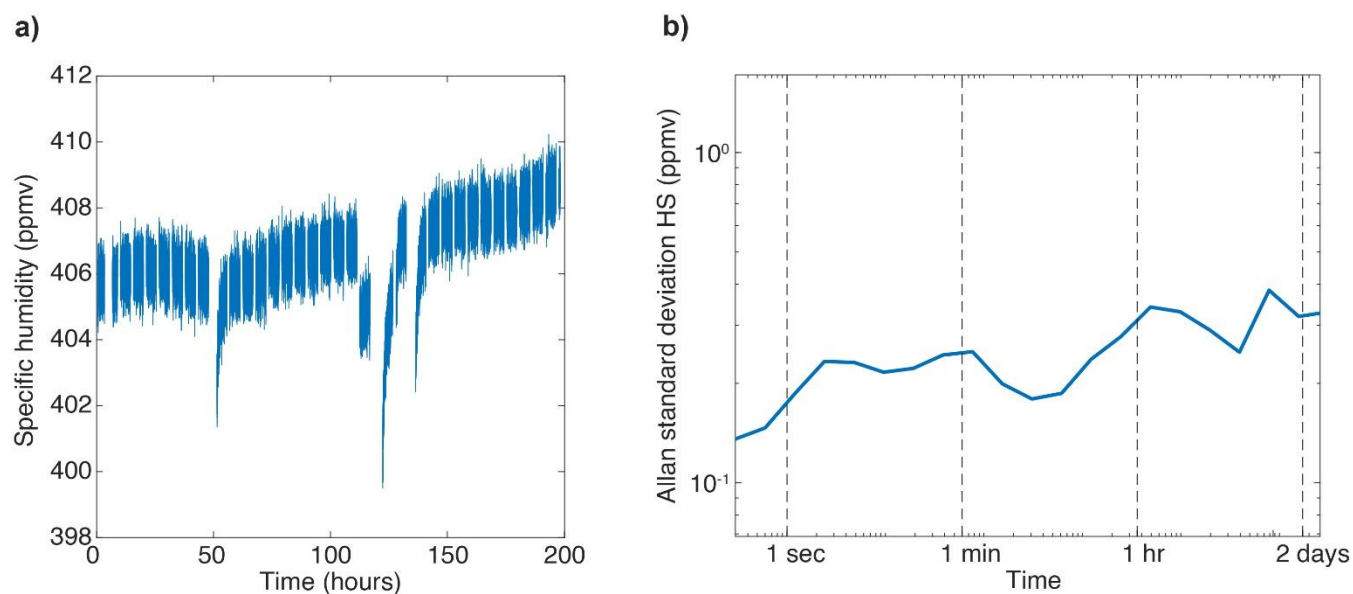
We build up a new infrared spectrometer based on relatively cheap telecom components hyped by high performances of optical feedback frequency stabilisation and cavity ring down spectroscopy. This new instrument demonstrates a precision and a stability of 0.01‰ for $\delta^{18}\text{O}$ and 0.1‰ for d-excess at extremely low humidities such as found in central Antarctica for duration
310 longer than 2 days. A key element to ensure limited drift even outside of the confine of a fully equipped spectroscopy lab is the use of the Lamb-dip feature as a frequency reference. This shows that the instrument is able to reach the same level of precision without any external validation of the frequency of the laser source. By supporting measurement down to 1 ppmv of humidity, this instrument shows great potential to finally be able to study the isotopic exchanges all year long in Antarctica where temperature can reach -80°C during the polar night.

315



Appendix A: Evaluation of the stability of the generated vapour levels

The humidity generator used here is based on the instrument described in (Leroy-Dos Santos et al., 2021). The humidity levels it generates, while extremely stable, are limited to a stability of roughly 20 ppmv over 1h. Due to the high precision of the infrared spectrometer discussed in this manuscript, it is possible that the drift observed on the isotopic composition here is linked with instability in the generated water humidity, and thus, isotopic composition associated with limited variations in the water and air inflow in the humidity generator. Figure A1a) shows the variations of humidity over the 8-day period that was used to produce the Allan standard deviation curve at 400 ppmv in Figure 4a. Over the course of 8 days, the measured humidity only varied by 10 ppmv, principally during refill of the syringe of the humidity generator (Leroy-Dos Santos et al., 2021). In addition, a drift of roughly 2.5 ppmv over the 8 days is visible on the time series. This drift is well visible on the Allan standard deviation plots (Fig. A1b). The very similar shape of the increase of the Allan standard deviation of specific humidity around 1 hour is very similar to the bump in the $\delta^{18}\text{O}$ Allan standard deviation (Fig. 4a) which suggests that the instability in the generated vapour sample could have created excess noise which is not linked with the spectrometer.

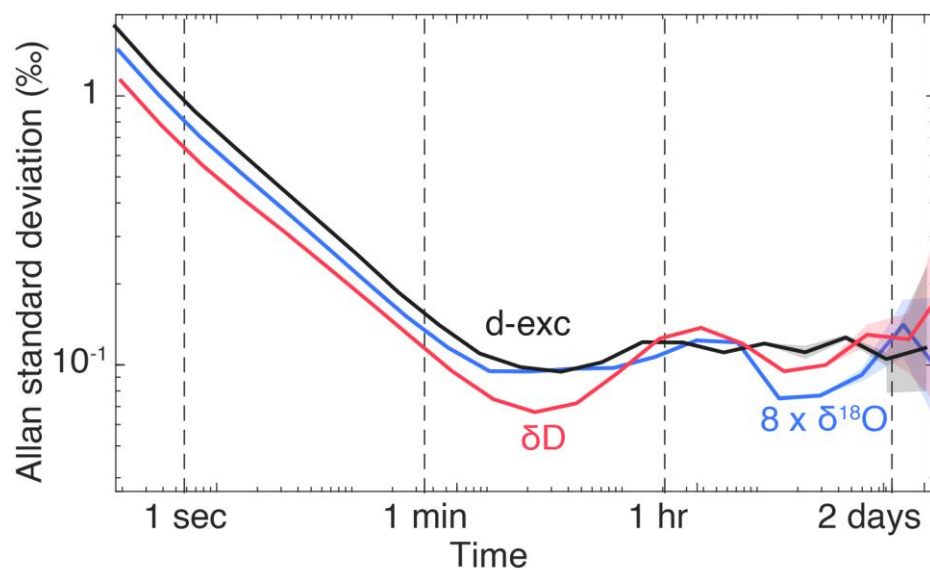


330 **Figure A1:** a) specific humidity time series during an 8-day monitoring of a stable isotopic sample, b) Allan standard deviation plots of the specific humidity measurements



Appendix B: Comparison of the Allan standard deviation of $\delta^{18}\text{O}$ and δD

335 Figure 4 and the result section focuses on $\delta^{18}\text{O}$ and d-excess because of the excess noise found in the $\delta^{18}\text{O}$ measurements due to the misalignment of the measurement point off the centre of the H_2^{18}O transition. In fact, we expect the drift of d-excess to be dominated by the drift of $\delta^{18}\text{O}$ due to the excess noise. Here, we show that this is relatively true at short time scales (below one hour, Fig. B1). At longer time scales, the excess noise from δD leads to a flat response of the d-excess Allan standard deviation.



340

Figure B1: Comparison of the Allan standard deviations of $\delta^{18}\text{O}$ (scaled by a factor 8 to ease the comparison), δD , and d-excess realised at 400 ppmv.



References

- 345 Akers, P. D., Kopec, B. G., Mattingly, K. S., Klein, E. S., Causey, D. and Welker, J. M.: Baffin Bay sea ice extent and synoptic moisture transport drive water vapor isotope ($\delta^{18}\text{O}$, $\delta^2\text{H}$, and deuterium excess) variability in coastal northwest Greenland, *Atmos. Chem. Phys.*, 20(22), 13929–13955, 2020.
- Bagheri Dastgerdi, S., Behrens, M., Bonne, J.-L., Hörhold, M., Lohmann, G., Schlosser, E. and Werner, M.: Continuous monitoring of surface water vapour isotopic compositions at Neumayer Station III, East Antarctica, *Cryosph.*, 15(10), 4745–
- 350 4767, 2021.
- Berkelhammer, M., Noone, D. C., Steen-Larsen, H. C., Bailey, A., Cox, C. J., O’Neill, M. S., Schneider, D., Steffen, K. and White, J. W. C.: Surface-atmosphere decoupling limits accumulation at Summit, Greenland, *Sci. Adv.*, 2(4), 2016.
- Bonne, J.-L., Behrens, M., Meyer, H., Kipfstuhl, S., Rabe, B., Schönicke, L., Steen-Larsen, H. C. and Werner, M.: Resolving the controls of water vapour isotopes in the Atlantic sector, *Nat. Commun.*, 10(1), 1–10, 2019.
- 355 Bonne, J. L., Masson-Delmotte, V., Cattani, O., Delmotte, M., Risi, C., Sodemann, H. and Steen-Larsen, H. C.: The isotopic composition of water vapour and precipitation in Ivittuut, southern Greenland, *Atmos. Chem. Phys.*, 14(9), 4419–4439, doi:10.5194/acp-14-4419-2014, 2014.
- Bréant, C., Dos Santos, C. L., Agosta, C., Casado, M., Fourré, E., Goursaud, S., Masson-Delmotte, V., Favier, V., Cattani, O. and Prié, F.: Coastal water vapor isotopic composition driven by katabatic wind variability in summer at Dumont d’Urville,
- 360 coastal East Antarctica, *Earth Planet. Sci. Lett.*, 514, 37–47, 2019.
- Burkart, J. and Kassl, S.: Absorption line metrology by optical feedback frequency-stabilized cavity ring-down spectroscopy, *Appl. Phys. B*, 119(1), 97–109, doi:10.1007/s00340-014-5999-3, 2015.
- Burkart, J., Romanini, D. and Kassl, S.: Optical feedback stabilized laser tuned by single-sideband modulation, *Opt. Lett.*, 38(12), 2062–2064, 2013.
- 365 Burkart, J., Romanini, D. and Kassl, S.: Optical feedback frequency stabilized cavity ring-down spectroscopy, *Opt. Lett.*, 39(16), 4695–4698, doi:10.1364/OL.39.004695, 2014.
- Burkart, J., Sala, T., Romanini, D., Marangoni, M., Campargue, A. and Kassl, S.: Communication: Saturated CO₂ absorption near 1.6 μm for kilohertz-accuracy transition frequencies, *J. Chem. Phys.*, 142(19), 191103, 2015.
- Casado, M.: Water stable isotopic composition on the East Antarctic Plateau: measurements at low temperature of the vapour
- 370 composition, utilisation as an atmospheric tracer and implication for paleoclimate studies, Paris Saclay., 2016.
- Casado, M.: Antarctic Stable Isotopes, in Reference Module in Earth Systems and Environmental Sciences, Elsevier., 2018.
- Casado, M., Landais, A., Masson-Delmotte, V., Genthon, C., Kerstel, E., Kassl, S., Arnaud, L., Picard, G., Prie, F., Cattani, O., Steen-Larsen, H. C., Vignon, E. and Cermak, P.: Continuous measurements of isotopic composition of water vapour on the East Antarctic Plateau, *Atmos. Chem. Phys.*, 16(13), 8521–8538, doi:10.5194/acp-16-8521-2016, 2016.
- 375 Casado, M., Landais, A., Picard, G., Münch, T., Laepple, T., Stenni, B., Dreossi, G., Ekaykin, A., Arnaud, L., Genthon, C., Touzeau, A., Masson-Delmotte, V. and Jouzel, J.: Archival processes of the water stable isotope signal in East Antarctic ice



- cores, *Cryosph.*, 12(5), 1745–1766, doi:10.5194/tc-12-1745-2018, 2018.
- Casado, M., Münch, T. and Laepple, T.: Climatic information archived in ice cores: impact of intermittency and diffusion on the recorded isotopic signal in Antarctica, *Clim. Past*, 16(4), 1581–1598, doi:10.5194/cp-16-1581-2020, 2020.
- 380 Casado, M., Landais, A., Picard, G., Arnaud, L., Dreossi, G., Stenni, B. and Prié, F.: Water isotopic signature of surface snow metamorphism in Antarctica, *Geophys. Res. Lett.*, e2021GL093382, 2021.
- Casado, M., Stoltmann, T., Landais, A., Jobert, N., Daëron, M., Prié, F. and Kassi, S.: High stability in near-infrared spectroscopy: part 1, adapting clock techniques to optical feedback, *Appl. Phys. B*, 128(3), 1–7, 2022.
- 385 Čermák, P., Karlovets, E. V., Mondelain, D., Kassi, S., Perevalov, V. I. and Campargue, A.: High sensitivity CRDS of CO₂ in the 1.74 μm transparency window. A validation test for the spectroscopic databases, *J. Quant. Spectrosc. Radiat. Transf.*, 207, 95–103, 2018.
- Chaillot, J., Dasari, S., Fleurbaey, H., Daeron, M., Savarino, J. and Kassi, S.: High-precision laser spectroscopy of H₂S for simultaneous probing of multiple-sulfur isotopes, *Environ. Sci. Adv.*, 2023.
- Craig, H. and Gordon, A.: Deuterium and oxygen 18 variations in the ocean and the marine atmosphere, *Stable Isot. Ocean. Stud. Paleotemp.*, 1(9), 130, 1965.
- 390 Dansgaard, W.: Stable isotopes in precipitation, *Tellus*, 16(4), 436–468, doi:10.1111/j.2153-3490.1964.tb00181.x, 1964.
- Ekaykin, A. A., Lipenkov, V. Y., Barkov, N. I., Petit, J. R. and Masson-Delmotte, V.: Spatial and temporal variability in isotope composition of recent snow in the vicinity of Vostok station, Antarctica: implications for ice-core record interpretation, *Ann. Glaciol.*, 35(1), 181–186, doi:10.3189/172756402781816726, 2002.
- 395 Ellehoj, M. D., Steen-Larsen, H. C., Johnsen, S. J. and Madsen, M. B.: Ice-vapor equilibrium fractionation factor of hydrogen and oxygen isotopes: Experimental investigations and implications for stable water isotope studies, *Rapid Commun. Mass Spectrom.*, 27(19), 2149–2158, doi:10.1002/rcm.6668, 2013.
- EPICA: Eight glacial cycles from an Antarctic ice core, *Nature*, 429(6992), 623–628 [online] Available from: <http://dx.doi.org/10.1038/nature02599>, 2004.
- 400 Galewsky, J., Steen-Larsen, H. C., Field, R. D., Worden, J., Risi, C. and Schneider, M.: Stable isotopes in atmospheric water vapor and applications to the hydrologic cycle, *Rev. Geophys.*, 54(4), 809–865, 2016.
- Genthon, C., Piard, L., Vignon, E., Madeleine, J.-B., Casado, M. and Gallée, H.: Atmospheric moisture supersaturation in the near-surface atmosphere at Dome C, antarctic plateau, *Atmos. Chem. Phys. Discuss.*, 2016, 1–37, doi:10.5194/acp-2016-670, 2016.
- 405 Genthon, C., Veron, D., Vignon, E., Six, D., Dufresne, J.-L., Madeleine, J.-B., Sultan, E. and Forget, F.: 10 years of temperature and wind observation on a 45 m tower at Dome C, East Antarctic plateau, *Earth Syst. Sci. Data*, 13(12), 5731–5746, 2021.
- Genthon, C., Veron, D. E., Vignon, E., Madeleine, J.-B. and Piard, L.: Water vapor in cold and clean atmosphere: a 3-year data set in the boundary layer of Dome C, East Antarctic Plateau, *Earth Syst. Sci. Data Discuss.*, 1–25, 2022.
- Gotti, R., Sala, T., Prevedelli, M., Kassi, S., Marangoni, M. and Romanini, D.: Feed-forward comb-assisted coherence transfer
410 to a widely tunable DFB diode laser, *J. Chem. Phys.*, 149(15), 154201, doi:10.1063/1.5046387, 2018.



- Izutsu, M., Shikama, S. and Sueta, T.: Integrated optical SSB modulator/frequency shifter, *IEEE J. Quantum Electron.*, 17(11), 2225–2227, 1981.
- Jobert, N., Casado, M. and Kassı, S.: High stability in near-infrared spectroscopy: part 2, optomechanical analysis of an optical contacted V-shaped cavity, *Appl. Phys. B*, 128(3), 56, doi:10.1007/s00340-022-07779-x, 2022.
- 415 Jouzel, J.: Institut Pierre Simon Laplace, Saclay, France, *Isot. Geochemistry A Deriv. Treatise Geochemistry*, 151, 2010.
- Jouzel, J. and Masson-Delmotte, V.: Paleoclimates: what do we learn from deep ice cores?, *Wiley Interdiscip. Rev. Clim. Chang.*, 1(5), 654–669, doi:10.1002/wcc.72, 2010.
- Kassı, S., Stoltmann, T., Casado, M., Daëron, M. and Campargue, A.: Lamb dip CRDS of highly saturated transitions of water near 1.4 μm , *J. Chem. Phys.*, 148(5), 54201, doi:10.1063/1.5010957, 2018.
- 420 Kurita, N., Hirasawa, N., Koga, S., Matsushita, J. and Fujiyoshi, Y.: Identification of air mass responsible for warm events at Syowa station, 2015.
- Laepple, T., Münch, T., Casado, M., Hoerhold, M., Landais, A. and Kipfstuhl, S.: On the similarity and apparent cycles of isotopic variations in East Antarctic snow pits, *Cryosph.*, 12(1), 169–187, doi:10.5194/tc-12-169-2018, 2018.
- Lamb, K. D., Clouser, B. W., Bolot, M., Sarkozy, L., Ebert, V., Saathoff, H., Möhler, O. and Moyer, E. J.: Laboratory
425 measurements of HDO/H₂O isotopic fractionation during ice deposition in simulated cirrus clouds, *Proc. Natl. Acad. Sci.*, 114(22), 5612–5617, 2017.
- Landsberg, J.: Development of an OF-CEAS laser spectrometer for water vapor isotope measurements at low water concentrations, University of Groningen., 2014.
- Landsberg, J., Romanini, D. and Kerstel, E.: Very high finesse optical-feedback cavity-enhanced absorption spectrometer for
430 low concentration water vapor isotope analyses, *Opt. Lett.*, 39(7), 1795–1798, doi:10.1364/OL.39.001795, 2014.
- Laurent, P., Clairon, A. and Breant, C.: Frequency noise analysis of optically self-locked diode lasers, *Quantum Electron. IEEE J.*, 25(6), 1131–1142, 1989.
- Leroy-Dos Santos, C., Casado, M., Prié, F., Jossoud, O., Kerstel, E., Farradèche, M., Kassı, S., Fourré, E. and Landais, A.: A dedicated robust instrument for water vapor generation at low humidity for use with a laser water isotope analyzer in cold and
435 dry polar regions, *Atmos. Meas. Tech.*, 14(4), 2907–2918, doi:10.5194/amt-14-2907-2021, 2021.
- Leroy - Dos Santos, C., Masson-Delmotte, V., Casado, M., Fourré, E., Steen-Larsen, H. C., Maturilli, M., Orsi, A., Berchet, A., Cattani, O. and Minster, B.: A 4.5 year-long record of Svalbard water vapor isotopic composition documents winter air mass origin, *J. Geophys. Res. Atmos.*, e2020JD032681, 2020.
- Long, D. A., Bielska, K., Lisak, D., Havey, D. K., Okumura, M., Miller, C. E. and Hodges, J. T.: The air-broadened, near-
440 infrared CO₂ line shape in the spectrally isolated regime: Evidence of simultaneous Dicke narrowing and speed dependence, *J. Chem. Phys.*, 135(6), 2011.
- Lorius, C., Merlivat, L. and Hagemann, R.: Variation in the mean deuterium content of precipitations in Antarctica, *J. Geophys. Res.*, 74(28), 7027–7031, doi:10.1029/JC074i028p07027, 1969.
- Majoube, M.: FRACTIONATION IN O-18 BETWEEN ICE AND WATER VAPOR, *J. Chim. Phys. Physico-Chimie Biol.*,



- 445 68(4), 625-- [online] Available from: %3CGo, 1971.
Merlivat, L. and Nief, G.: Fractionnement isotopique lors des changements d'état solide-vapeur et liquide-vapeur de l'eau à des températures inférieures à 0°C, *Tellus*, 19(1), 122–127, doi:10.1111/j.2153-3490.1967.tb01465.x, 1967.
Morville, J., Kassi, S., Chenevier, M. and Romanini, D.: Fast, low-noise, mode-by-mode, cavity-enhanced absorption spectroscopy by diode-laser self-locking, *Appl. Phys. B*, 80(8), 1027–1038, doi:10.1007/s00340-005-1828-z, 2005.
- 450 North Greenland Ice Core Project members: High-resolution record of Northern Hemisphere climate extending into the last interglacial period, *Nature*, 431(7005), 147–151 [online] Available from: <http://dx.doi.org/10.1038/nature02805>, 2004.
Risi, C., Bony, S. and Vimeux, F.: Influence of convective processes on the isotopic composition ($\delta^{18}\text{O}$ and $\delta^2\text{H}$) of precipitation and water vapor in the tropics: 2. Physical interpretation of the amount effect, *J. Geophys. Res. Atmos.*, 113(D19), D19306, doi:10.1029/2008JD009943, 2008.
- 455 Ritter, F., Steen-Larsen, H. C., Werner, M., Masson-Delmotte, V., Orsi, A., Behrens, M., Birnbaum, G., Freitag, J., Risi, C. and Kipfstuhl, S.: Isotopic exchange on the diurnal scale between near-surface snow and lower atmospheric water vapor at Kohnen station, East Antarctica, *Cryosph.*, 2016, 1–35, doi:10.5194/tc-2016-4, 2016.
Romanini, D., Kachanov, A. A., Sadeghi, N. and Stoeckel, F.: CW cavity ring down spectroscopy, *Chem. Phys. Lett.*, 264(3–4), 316–322, doi:[http://dx.doi.org/10.1016/S0009-2614\(96\)01351-6](http://dx.doi.org/10.1016/S0009-2614(96)01351-6), 1997.
- 460 Steen-Larsen, H. C., Johnsen, S. J., Masson-Delmotte, V., Stenni, B., Risi, C., Sodemann, H., Balslev-Clausen, D., Blunier, T., Dahl-Jensen, D., Ellehøj, M. D., Falourd, S., Grindsted, A., Gkinis, V., Jouzel, J., Popp, T., Sheldon, S., Simonsen, S. B., Sjolte, J., Steffensen, J. P., Sperlich, P., Sveinbjörnsdóttir, A. E., Vinther, B. M. and White, J. W. C.: Continuous monitoring of summer surface water vapor isotopic composition above the Greenland Ice Sheet, *Atmos. Chem. Phys.*, 13(9), 4815–4828, doi:10.5194/acp-13-4815-2013, 2013.
- 465 Steen-Larsen, H. C., Masson-Delmotte, V., Hirabayashi, M., Winkler, R., Satow, K., Prié, F., Bayou, N., Brun, E., Cuffey, K. M. and Dahl-Jensen, D.: What controls the isotopic composition of Greenland surface snow?, *Clim. Past*, 10(1), 377–392, 2014.
Steig, E. J., Gkinis, V., Schauer, A. J., Schoenemann, S. W., Samek, K., Hoffnagle, J., Dennis, K. J. and Tan, S. M.: Calibrated high-precision ^{17}O -excess measurements using cavity ring-down spectroscopy with laser-current-tuned cavity resonance, *Atmos. Meas. Tech.*, 7(8), 2421–2435, doi:10.5194/amt-7-2421-2014, 2014.
- 470 Stoltmann, T., Casado, M., Daëron, M., Landais, A. and Kassi, S.: Direct, Precise Measurements of Isotopologue Abundance Ratios in CO_2 Using Molecular Absorption Spectroscopy: Application to $\Delta^{17}\text{O}$, *Anal. Chem.*, 89(19), 10129–10132, 2017.
Thurnherr, I., Kozachek, A., Graf, P., Weng, Y., Bolshiyarov, D., Landwehr, S., Pfahl, S., Schmale, J., Sodemann, H. and Steen-Larsen, H. C.: Meridional and vertical variations of the water vapour isotopic composition in the marine boundary layer over the Atlantic and Southern Ocean, *Atmos. Chem. Phys.*, 20(9), 5811–5835, 2020.
Wei, Z., Lee, X., Aemisegger, F., Benetti, M., Berkelhammer, M., Casado, M., Caylor, K., Christner, E., Dyroff, C. and García, O.: A global database of water vapor isotopes measured with high temporal resolution infrared laser spectroscopy, *Sci. data*, 6(1), 1–15, 2019.



480 Weng, Y., Touzeau, A. and Sodemann, H.: Correcting the impact of the isotope composition on the mixing ratio dependency
of water vapour isotope measurements with cavity ring-down spectrometers, *Atmos. Meas. Tech.*, 13(6), 3167–3190, 2020.

Werner, M., Langebroek, P. M., Carlsen, T., Herold, M. and Lohmann, G.: Stable water isotopes in the ECHAM5 general
circulation model: Toward high-resolution isotope modeling on a global scale, *J. Geophys. Res. Atmos.*, 116(D15), D15109,
doi:10.1029/2011JD015681, 2011.

485 **Author contributions.** *AL and SK organised the project, MC, TS, JC and SK built the instrument, FP and BB support the
project and the measurements, MC wrote the manuscript with help of all the co-authors.*

Competing interests. *The authors declare that they have no conflict of interest.*

490 **Acknowledgments.** *The research leading to these results has received funding from the European Research Council under the
European Union’s Seventh Framework Programme (FP7/2007- 2013)/RC grant agreement number 306045. We thank Erik
Kerstel, Daniele Romanini, Johannes Burkart, and Peter Cermak for our fruitful discussions which helped improve the
manuscript.*